INTERNATIONAL JOURNAL FOR NUMERICAL METHODS IN FLUIDS, VOL. 16, 29–42 (1993)

DIE DESIGN: AN IMPLICIT FORMULATION FOR THE INVERSE PROBLEM

VINCENT LEGAT

Applied Mechanics, Université Catholique de Louvain, 2 Place du Levant, B-1348 Louvain-la-Neuve, Belgium

AND

JEAN-MARIE MARCHAL

Polyflow S.A., 16 Place de l'Université, B-1348 Louvain-la-Neuve, Belgium

SUMMARY

Let us call a direct extrusion problem (DEP) the problem of finding the shape of the extrudate coming out of a die of prescribed shape. An implicit finite element formulation of the DEP which is geometrically general and for which a Newton–Raphson technique can be implemented has recently been proposed by Legat and Marchal. However, the problem posed to the die designer is frequently the inverse extrusion problem (IEP), i.e. finding the die shape which produces an extrudate of prescribed shape. This paper presents an extension of our original method for solving the IEP which avoids the 'trial-and-error' iteration on the die geometry itself.

The advantage of the formulation lies in its capability to handle complex geometries and in its low cost, because the CPU time and memory required to solve the IEP are almost identical to those of the DEP. We present benchmark results for squares and rectangles and new results obtained for geometries involving multiple corners. For an octagonal shape we also consider the case of a power-law fluid.

For all results presented in this paper, surface tension has not been included.

KEY WORDS 3D extrusion Moving boundaries Die design Remeshing Finite elements Free surfaces

1. INTRODUCTION

Let us consider a free surface flow problem in a three-dimensional geometry. For the sake of simplicity the flow is assumed to be isothermal and the fluid is Newtonian. Let us assume that an algorithm is available to solve the direct extrusion problem (DEP). If the extrudate shape does not correspond to the desired profile, the die designer will naturally adapt the geometry of the die in order to correct the extrudate shape. An outer iteration (above the solution of the DEP) will be introduced and the die geometry will be modified according to the designer's intuition or on the basis of an interpolation between the prescribed shape and the simulation result.

This inverse extrusion problem (IEP) is so important from a technical point of view that many authors who presented numerical solutions for the DEP[1–4] also considered the IEP. In Reference 2 an outer iteration on the die geometry above the solution of the DEP has been introduced. In References 1, 3 and 4 the use of an outer iteration on the free surface position itself (streamline integration) allows for an inverse tracking of the characteristics ($\mathbf{v}$ for the DEP, $-\mathbf{v}$ for the IEP). For this backward tracking the prescribed extrudate shape becomes a boundary condition of the

0271–2091/93/010029–14$12.00

Received 28 January 1992
Revised 5 August 1992

problem. However, difficulties occur near the die lip, where the fluid velocity is imposed to be zero. In an implicit technique based on a Galerkin (or a streamline upwind/Petrov–Galerkin) formulation of the kinematic condition, removing the initial data of the kinematic condition at the die lip makes the tangent matrix singular and prevents the use of the method.

In order to formulate the IEP correctly in terms of velocity, pressure and displacement, we replace the initial data on the free surface at the die lip by the constraint that the shape of the extrudate is prescribed at the end of the free surface. The method is inspired by a technique frequently used in the field of numerical solutions of ODEs. To illustrate our method, let us consider a second-order ODE written as

find $f(x)$ such that

$$\ddot{f}(x)=A(f(x)) \quad \forall x\in[0,1]. \tag{1}$$

Equation (1) is subject to two boundary conditions, which can be given at both ends of the interval or at one end only. Let us assume that we want to solve (1) numerically subject to the conditions

$$f(0)=f_0, \tag{2}$$

$$f(1)=f_1 \tag{3}$$

and that we use a numerical technique which requires f and $\dot{f}$ in $x=0$. This case occurs for example with most methods of the Runge–Kutta family, which have the advantage of not requiring one to solve a linear system. A classical way to solve (1) subject to (2) and (3) is then to estimate the value of $\dot{f}(0)$ and to use a shooting method in order to satisfy (3) at convergence of the algorithm. An alternative is to introduce the value of $\dot{f}(0)$ as a variable of the problem (in the previous formulation $\dot{f}(0)$ is a datum) and to write the constraint (3) as an equation for $\dot{f}(0)$. In this method the new variable which replaces the datum $\dot{f}(0)$ is a multiplier; this numerical technique is cost-effective with respect to the shooting method, because the additional variable can be eliminated algebraically.

Our method is inspired by the scheme described above, provided that one replaces the datum $\dot{f}(0)$ by the initial position of the free surface at the die lip and introduces a smooth variation of the die shape in the direction of extrusion in order to look for a solution of the IEP in a class of technically acceptable dies. This method is certainly cost-effective for the IEP formulated in terms of velocity, pressure and displacement, because the number of velocity and pressure variables is superior to the number of position variables, which is in turn superior to the number of multipliers required to describe the die section.

Strictly speaking, the new variable is not a Lagrange multiplier because we do not solve a constrained optimization problem. However, it is impossible to formulate a free surface problem in the Lagrangian sense.[5]

However, in the extended sense we consider the new variable as a multiplier which has been introduced in order to weakly impose the boundary condition at the exit. A similar approach has previously be used in free surfaces problems in order to weakly impose kinematic and dynamic conditions.[6,7] In view of the impossibility of formulating the Navier–Stokes equations with free surfaces in a variational sense as a minimum problem, we consider its extension based on a Galerkin formulation. Indeed, this definition of the multipliers is inspired by the general optimization approach.

Section 2 formulates the IEP and introduces a finite element representation, while Section 3 presents the remeshing techniques used in order to minimize mesh deformations. In Sections

4 and 5 we describe benchmark results for square and rectangular geometries. Then we demonstrate the robustness of the method for several geometries involving abrupt corners.

2. FORMULATION OF THE INVERSE EXTRUSION PROBLEM

We simulate steady three-dimensional isothermal free surface flows of a Newtonian fluid (or a generalized Newtonian fluid). Let Ω be the flow domain, with boundary $\partial\Omega$. The geometry of the problem is schematically defined in Figure 1, which is two-dimensional for the sake of clarity, although all problems presented in this paper are three-dimensional.

Let $(\mathbf{v}, p)$ be respectively the velocity and pressure of the problem, elements of the function space $V \times P$ defined on the flow domain Ω. Let h be the amplitude of the displacement of the free surface $\partial\Omega_{\text{Free}}$ along the **d**-direction, so that the displacement $\delta\mathbf{x}$ of a point of the free surface is given by

$$\delta\mathbf{x} = h\mathbf{d} \qquad \text{on } \partial\Omega_{\text{Free}}. \tag{4}$$

The direction **d** can vary from point to point in order to describe the displacement allowed to the free surface, but **d** is given *a priori* and is not a variable of the problem. In practice, **d** is calculated as the normal to the initial guess of the free surface. Functions h belong to a function space H. Along lines of discontinuities of the normal, two directions d_i and two amplitudes h_i are defined in order to correctly handle the motion of corners. The double definition allows corners to move freely in the planes orthogonal to the direction of extrusion. More precisely, we do not consider one field h but a series of fields h_i belonging to a series of function spaces H_i limited to 'faces' of the free surface, as explained in Reference 8. Let $\partial\Omega_{\text{Die}}$ be the die boundary itself, on which a zero velocity is prescribed, and let C_{Lip} be the curve representing the die lip. Let C_{Exit} be the curve located at the intersection between the free surface and the outlet section. We introduce a generalized Lagrange multiplier g belonging to G, which is a space of functions defined over C_{Exit}. The function g defines the shape of the die and is adapted in order to satisfy the constraint on the extrudate shape on C_{Exit} at the end of the free surface. If C_{Exit} and C_{Lip} are topologically identical, the deformation of the die shape can be naturally defined as

$$\delta\mathbf{x} = f(z)g\mathbf{d} \qquad \text{on } \partial\Omega_{\text{Die}}. \tag{5}$$

In (5), z represents the direction of extrusion and we have introduced the hypothesis of proportional adaptation in the z-direction. The die design function $f(z)$ is of course a datum of the problem and describes the transition between the prescribed inlet section and the die lip. To

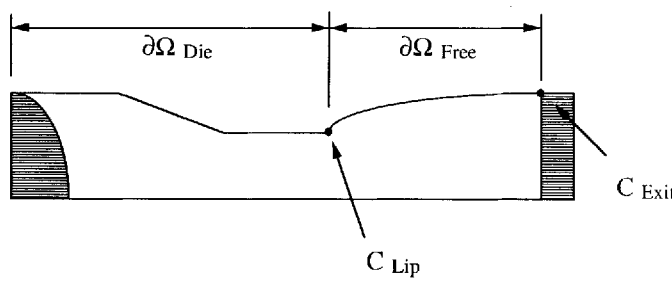

Figure 1. Configuration of the extrusion die and of the extrudate

illustrate (5), let us consider cases a, b and c in Figure 2. The function $f(z)$ is defined as

$$\begin{aligned} f(z)&=0 && \text{on } [z_1, z_2],\\ f(z)&=\frac{z-z_2}{z_3-z_2} && \text{on } [z_2, z_3],\\ f(z)&=1 && \text{on } [z_3, z_4], \end{aligned} \tag{6}$$

with $z_1 \leqslant z_2 \leqslant z_3 \leqslant z_4$.

In case 'a' z_2, z_3 and z_4 are not identical. For case 'b' $z_3 = z_4$ and for case 'c' $z_2 = z_3$. It must be noted that z_1 cannot be equal to z_2 if we want to have compatibility between the die modification and the imposed inlet velocity profile. It is clear that the die functions can be more complex in order to consider more sophisticated dies. There is, however, a topological limitation: the number of nodes on C_{Exit} and C_{Lip} must be equal.

If the flow domain boundary $\partial\Omega$ is partitioned into $\partial\Omega_{\text{Dirichlet}}$ (the boundary part on which Dirichlet boundary conditions apply) and $\partial\Omega_{\text{Neumann}}$ (the boundary part on which homogeneous Neumann boundary conditions apply), the DEP and IEP are respectively formulated as

DEP: find $(\mathbf{v}, p, h) \in V \times P \times H$ such that

$$\nabla \cdot (\eta \bar{\nabla} \mathbf{v}) - \nabla p = 0 \quad \text{on } \Omega, \tag{7}$$

$$\nabla \cdot \mathbf{v} = 0 \quad \text{on } \Omega, \tag{8}$$

$$\mathbf{v} \cdot \mathbf{n} = 0 \quad \text{on } \partial\Omega_{\text{Free}}, \tag{9}$$

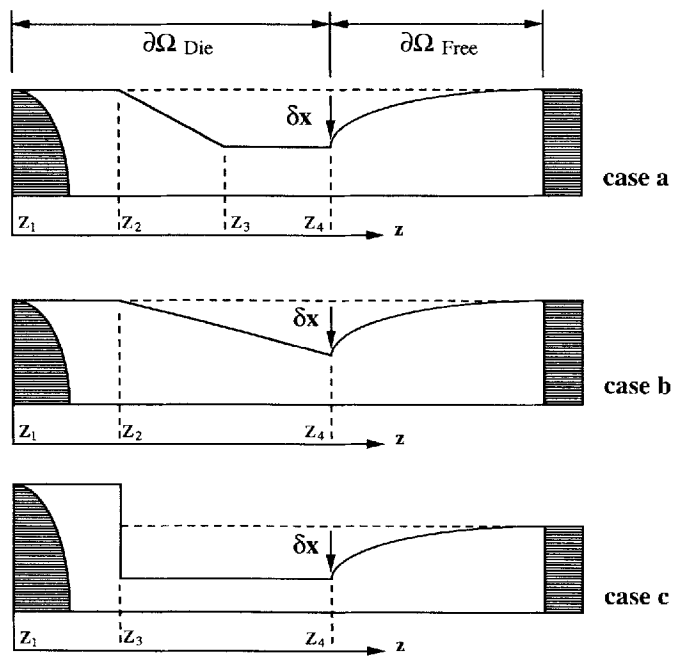

Figure 2. Die design functions for the adaptative die section

together with

$$h=0 \quad \text{on } C_{\text{Lip}}, \tag{10}$$

$$\mathbf{v}=\hat{\mathbf{v}} \quad \text{on } \partial\Omega_{\text{Dirichlet}}, \tag{11}$$

$$(\eta\bar{\nabla}\mathbf{v}-p\mathbf{I})\cdot\mathbf{n}=0 \quad \text{on } \partial\Omega_{\text{Neumann}}; \tag{12}$$

IEP: find $(\mathbf{v}, p, h, g)\in V\times P\times H\times G$ such that

$$\nabla\cdot(\eta\bar{\nabla}\mathbf{v})-\nabla p=0 \quad \text{on } \Omega, \tag{13}$$

$$\nabla\cdot\mathbf{v}=0 \quad \text{on } \Omega, \tag{14}$$

$$\mathbf{v}\cdot\mathbf{n}=0 \quad \text{on } \partial\Omega_{\text{Free}}, \tag{15}$$

$$h=0 \quad \text{on } C_{\text{Exit}}, \tag{16}$$

together with

$$h=g \quad \text{on } C_{\text{Lip}}, \tag{17}$$

$$\mathbf{v}=\mathbf{v} \quad \text{on } \partial\Omega_{\text{Dirichlet}}, \tag{18}$$

$$(\eta\bar{\nabla}\mathbf{v}-p\mathbf{I})\cdot\mathbf{n}=0 \quad \text{on } \partial\Omega_{\text{Neumann}}; \tag{19}$$

where $\bar{\nabla}\mathbf{v}$ denotes the symmetric part of the velocity gradient, η is the fluid viscosity and $\mathbf{n}$ is the unit normal vector pointing out of the domain Ω.

In the IEP, equation (16) guarantees that the extrudate shape matches the prescribed shape which is given as the initial guess *and is the equation for g*. Equation (17) replaces the data at the die lip *and is written as a constraint on h*. It must be noted that equation (17) is a valid boundary condition only if C_{Lip} and C_{Exit} are topologically identical. In addition, standard Neumann and Dirichlet boundary conditions apply in the entry section where a fully developed velocity profile is imposed, on planes of symmetry and on the die wall where the velocity vector is imposed as zero.

The IEP finite element formulation is derived from equations (13)–(19), after integration by Green's theorem of equation (13), so that Neumann boundary conditions appear naturally. The spaces V^h, P^h, H^h and G^h being appropriate approximation subspaces for V, P, H and G, the discrete IEP is formulated as

Find $(\mathbf{v}^h, p^h, h^h, g^h)\in V^h\times P^h\times H^h\times G^h$ such that

$$\langle\eta\bar{\nabla}\mathbf{v}-p\mathbf{I};\bar{\nabla}\mathbf{w}\rangle=0 \quad \forall\mathbf{w}\in V^h, \tag{20}$$

$$\langle\nabla\mathbf{v};q\rangle=0 \quad \forall q\in P^h, \tag{21}$$

$$\langle\mathbf{v}\cdot\mathbf{n};k\rangle=0 \quad \forall k\in H^h, \tag{22}$$

$$\langle h;l\rangle=0 \quad \forall l\in G^h. \tag{23}$$

In equations (20)–(23), $\langle\cdot\rangle$ stands for the L_2 scalar product on Ω, $\partial\Omega_{\text{Free}}$ or C_{Exit}; the space V^h takes the Dirichlet boundary conditions (18) into account and the displacement h is constrained by g at the lip of the extrusion die.

As in any saddle-point problem, interpolation subspaces V^h, P^h, H^h and G^h cannot be selected arbitrarily. Interpolations must satisfy the so-called Ladyzhenskaya–Brezzi–Babuska (LBB) conditions. Indeed, these discrete LBB conditions can be seen as a critical requirement in the stability of mixed finite element methods. For V^h and P^h we have selected the Q_2–C_0/Q_1–C_0 element (or the Q_1–C_0/Q_0–C_1 element). The selection of shape functions for H^h is somewhat

more difficult, since no theoretical results are available for this non-linear problem. In the absence of surface tension we have observed that the linear approximation for H^h works better than the quadratic one, in the sense that wiggles in the free surface and divergence of the iterative scheme have sometimes been observed with quadratic shape functions. However, all results of Sections 4 and 5 have been obtained with both bilinear and biquadratic position shape functions. Functions in G^h are equal to the restriction on the die exit C_{Exit} of functions of H^h, i.e. these functions are either piecewise linear or piecewise quadratic. The approximation subspaces H^h and G^h are finally divided into N_F faces, generating H_i^h and G_i^h, to take into account the presence of corners. This procedure is explained in Reference 8.

3. REMESHING

The position of the boundary comes into (20)–(23) by means of the relation (4) on the free surface $\partial\Omega_{\text{Free}}$ and (5) on the die boundary $\partial\Omega_{\text{Die}}$. In order to have acceptable mesh deformations, it is necessary to adapt the position of the interior nodes as a function of the boundary nodes. If we use a linear relationship between the displacements of the interior and boundary nodes, the remeshing of the interior nodes can be coupled to the system and a full Newton–Raphson technique can be derived.

In all examples we have used the remeshing rule developed in Reference 8, which is based on the Euclidean distance between the boundary nodes and the interior nodes. This remeshing rule is applied in the whole flow domain Ω and is implemented as follows.

Firstly, we divide Ω into a series of 'planes', logically orthogonal to the direction of extrusion. Interior nodes belong to one and only one planar section Ω_R and the traces in each plane of the three-dimensional mesh are topologically identical.

Secondly, a one-dimensional remeshing rule is used on boundary segments $\partial\Omega_R$ of each plane Ω_R, such that the points are moved tangentially as a linear function of the displacement of the extremities of the segment.

Finally, a Euclidean distance rule relates the interior displacements to the boundary displacements in each remeshing section Ω_R. The position of an interior node $\mathbf{x}_i$ is formally written as

$$\mathbf{x}_i^{\text{new}} = \mathbf{x}_i^0 + \sum_{j=1,N} w_{ij}(\mathbf{x}_j^{\text{new}} - \mathbf{x}_j^0), \tag{24}$$

where j is an index describing the two segment extremities (for a one-dimensional rule on $\partial\Omega_R$) or all nodes located on $\partial\Omega_R$ (for a two-dimensional rule on Ω_R). The weight w_{ij} is a function of the Euclidean distance between node i and node j:

$$w_{ij} = \frac{\sum_{k=1,N} |\mathbf{x}_i^0 - \mathbf{x}_k^0|_2}{N|\mathbf{x}_i^0 - \mathbf{x}_j^0|_2}. \tag{25}$$

This rule has the advantage of not requiring any particular logical organization of the mesh into each remeshing section Ω_R. In addition, the Euclidean distance remeshing rule associated with the priority rule allows us to deform the mesh smoothly. These rules are described in Reference 8.

4. A BENCHMARK PROBLEM: THE SQUARE SECTION

Computing the die geometry which produces a square profile is a benchmark problem which has been considered by Tran-Cong and Phan-Thien,[1] Yokoi and Scriven[3] and Wambersie and Crochet.[2] We have tested our technique on this problem with meshes I–III, for which the die

design function is described by

$$z_1=0, \qquad z_2=2, \qquad z_3=6, \qquad z_4=8.$$

In order to evaluate the effect of the upstream geometry on the extrudate shape, we have also generated meshes IV–VI, which correspond to the die design function

$$z_1=0, \qquad z_2=z_3=4, \qquad z_4=6.$$

The die length is equal to 8 for meshes I–III and 6 for meshes IV–VI. The extrudate length is 4 for all meshes. The square section (final product) has a side length equal to 2. The inflow geometry of meshes IV–VI has a side length equal to 4 and is also identical to the geometry used by Wambersie and Crochet[2]. Figures 3 and 4 show the meshes while Figure 5 shows the die lip section and the final extrudate section for meshes I–III.

In order to quantitatively evaluate the swelling effect, we introduce the swelling ratio along the plane of symmetry, Sw_m, and the diagonal swelling ratio Sw_d. Referring to Figure 6, let $2M$ and $2D$ be respectively the side and diagonal of the square extrudate profile. We define the length of the die in the planes of symmetry at the die lip by $2m$, whereas the diagonal of the die is defined by $2d$. The swelling ratios are defined as

$$Sw_m=(M-m)/M,$$

$$Sw_d=(D-d)/D.$$

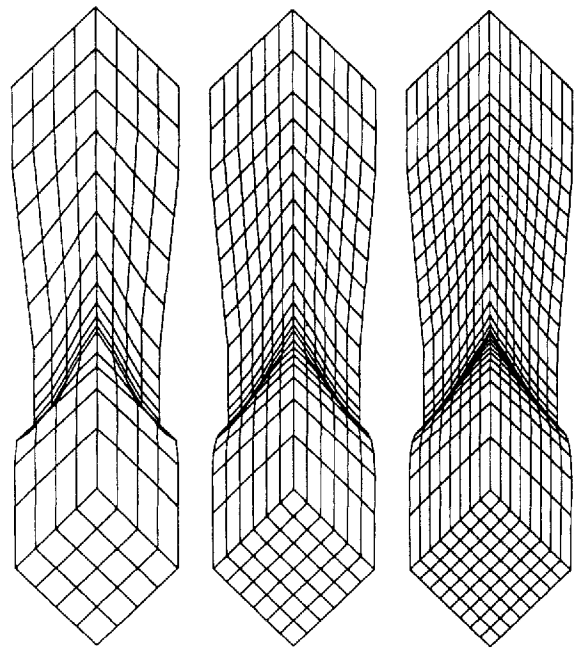

mesh I mesh II mesh III

Figure 3. Finite element meshes I–III used for testing the accuracy of the method (square extrudate)

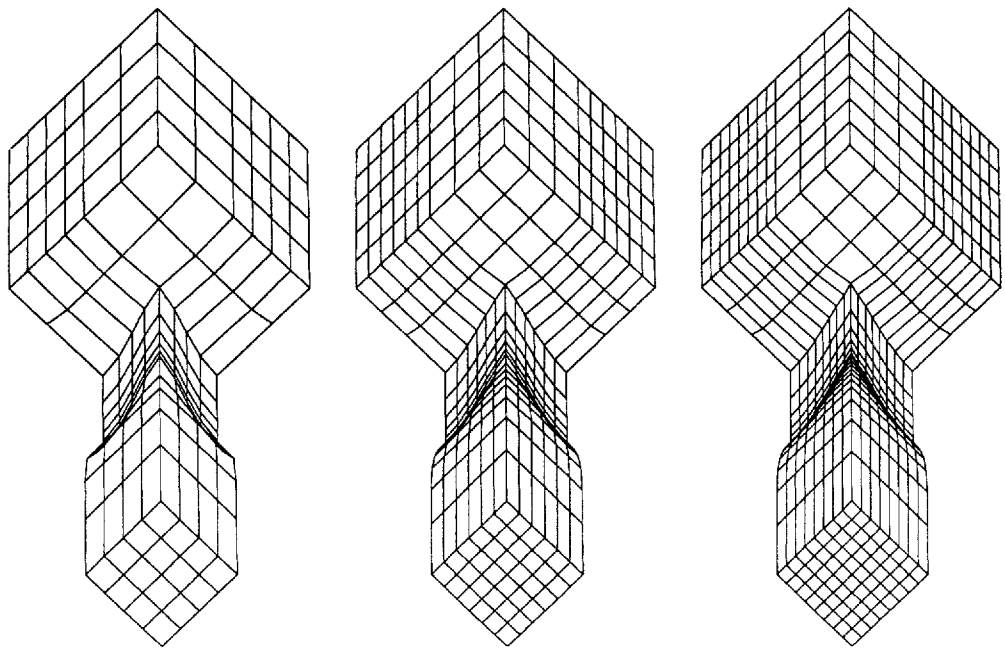

mesh IV mesh V mesh VI

Figure 4. Finite element meshes IV–VI used for testing the accuracy of the method (square extrudate)

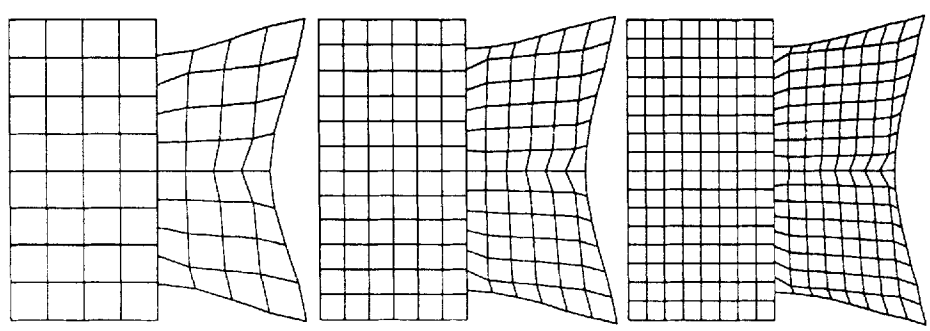

mesh I mesh II mesh III

Figure 5. Comparison between the die lip and the extrudate section for meshes I–III

Table I reports the total number of variables in the problem and the swelling ratios. It appears from Table I and Figure 7 that the convergence with mesh refinement is excellent between meshes II and III. Meshes I and IV are coarse, but their results are qualitatively good. The results for meshes IV–VI agree exactly with the results for meshes I–III although the die function is different

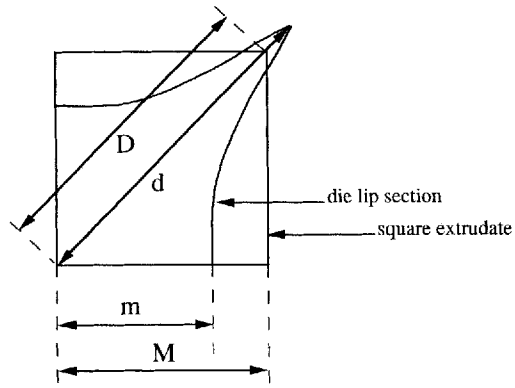

Figure 6. Typical dimensions for the square extrudate

Table I

Mesh	Nodes	Elements	Degrees of freedom	Sw_m	Sw_d
I	425	256	1041	0·236	−0·004
II	1078	756	3110	0·190	−0·017
III	2187	1664	6851	0·179	−0·021
VI	2304	1750	7058	0·179	−0·021
V	1237	873	3455	0·190	−0·017
IV	495	304	1113	0·237	−0·004

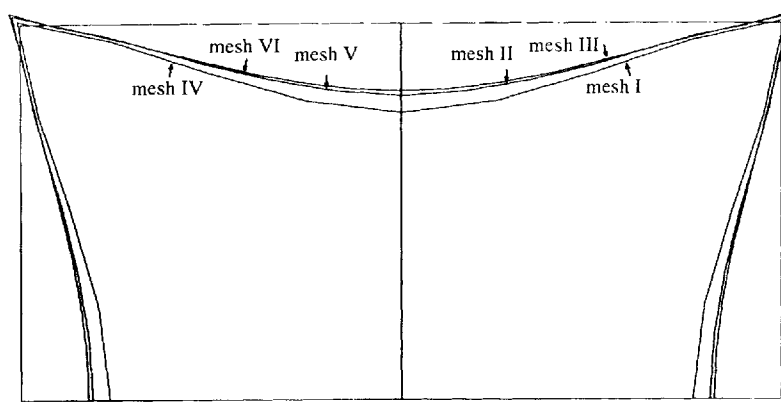

Figure 7. Mesh refinement analysis for the square extrudate

in the latter cases. This can be explained because the length of the constant shape section, $z_4 - z_3$, is equal to 2 for both meshes, and the upstream section has very little influence on the extrudate shape as long as $z_4 - z_3$ is bigger than a typical dimension of the section. We have found that a length of 2 is perfectly adequate in order to avoid dependences of the extrudate shape on the upstream geometry.

The results of Tran-Cong and Phan-Thien[1] have not been included in Table I, because they used die functions for which $z_4 - z_3 = 0$ (i.e. a linear variation up to the die lip), in which case the shape of the upstream section has a strong influence on the swelling. Yokoi and Scriven[3] and Wambersie and Crochet[2] do not mention numerical values, but their shapes agree graphically with ours.

These solutions converge quadratically up to a relative precision of 10^{-6} in five or six iterations.

5. NUMERICAL RESULTS FOR COMPLEX GEOMETRIES

5.1. Rectangular profiles

For a Newtonian fluid we report on die sections which produce rectangular extrudates for different aspect ratios. As a difference from the square section, an appropriate definition of two geometrical degrees of freedom around the corner is essential, since one does not know *a priori* in which direction the corner will move.

In all cases the die function has been chosen as

$$z_1 = 0, \qquad z_2 = 2, \qquad z_3 = 6, \qquad z_4 = 8.$$

A comparison between the extrudate shape (left) and the die section shape (right) is given in Figure 8. Quadratic convergence of the iteration scheme has been observed.

5.2. Octagonal profile

Most polymers present a shear-thinning behaviour which can be described by a dependence of the viscosity η on the shear rate $\dot{\gamma}$ of the power-law type:

$$\eta(\dot{\gamma}) = \eta_0 \dot{\gamma}^{m-1}.$$

This is valid as long as memory effects are not dominant. For a Newtonian fluid the power-law index is equal to 1, whereas for many polymers it lies between 0·5 and 0·2. We know that in the

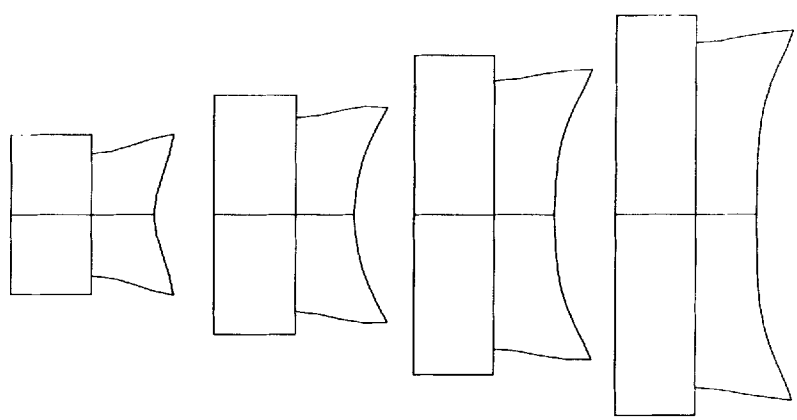

Figure 8. Cross-sections of dies (right) for generating rectangular extrudates (left)

presence of a low power-law index the velocity distribution will be relatively flat across the die section, a large velocity gradient existing near the wall of the die where the velocity vanishes. This velocity distribution will reduce swelling effects. We have analysed the shape of the die section which produces an octagonal extrudate for $m = 1, 0{\cdot}8, 0{\cdot}6, 0{\cdot}4$ and $0{\cdot}2$. Let us also emphasize that the no-slip boundary condition has been used at the die wall and that this hypothesis is probably not verified in many extrusion applications.

The octagon side being equal to 1, we have used the following die function:

$$z_1 = 0, \qquad z_2 = 2, \qquad z_3 = 6, \qquad z_4 = 8.$$

The total die length is equal to 8, the extrudate length being equal to 4. The mesh used for these simulations is shown in Figure 9. We have used symmetry with respect to the planes $x = 0$ and $x = y$ and discontinuity of the direction **d** has been used for the corner. Die section shapes are reported in Figure 10 for the different values of the power-law index. It can be observed that the

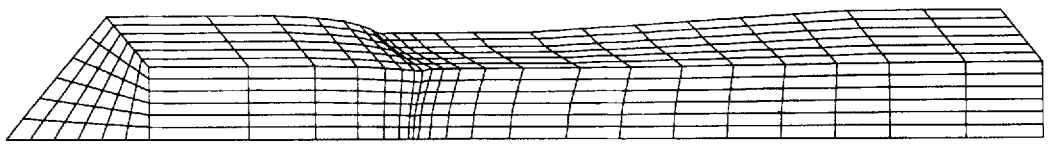

Figure 9. Finite element mesh used for the octagonal extrudate

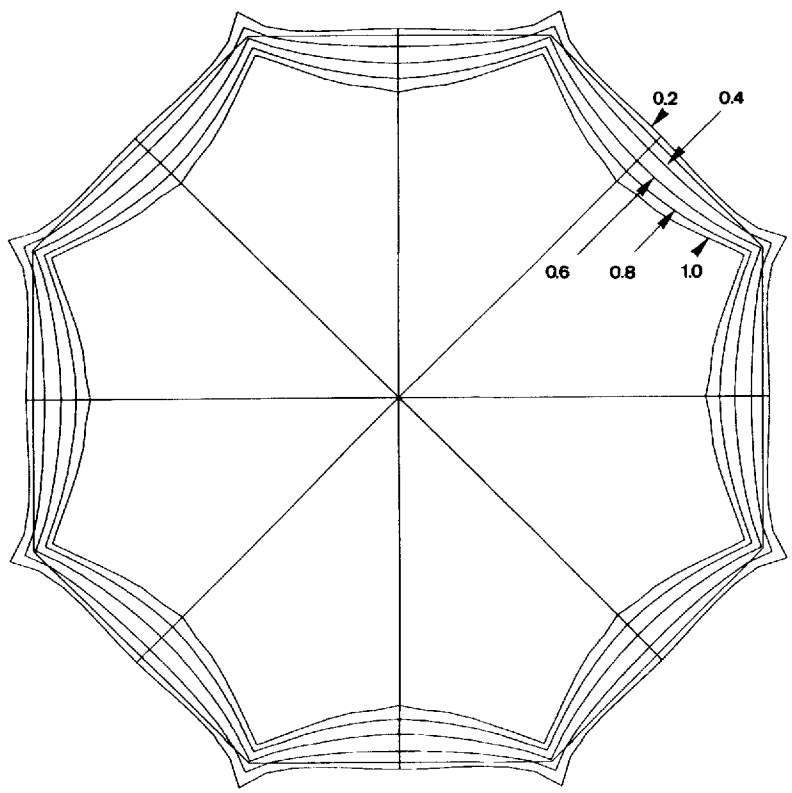

Figure 10. Die cross-sections as a function of the power-law index for the octagonal extrudate

shear-thinning behaviour indeed reduces the swelling but that the effect of the corner remains important even for low values of the power-law index. For very low values of the power-law index (0·3 and lower), sharp velocity boundary layers require meshes finer than the mesh shown in Figure 9 and a Picard iteration scheme on $\eta(\dot{\gamma})$ must be used to obtain results at $m=0{\cdot}2$. However, a full Newton–Raphson scheme can be used for the indices between 1 and 0·4, in which case a quadratic convergence is observed.

To understand the effect of the uniformity of the velocity distribution on the swelling, contour lines of the normal velocity are shown in Figure 11 for different power-law indices.

5.3. Star-like profile

For a Newtonian fluid the die section which produces a 'star-like' extrudate is shown in Figure 12. Shrinkage effects are large near the re-entrant corner A, where two geometrical degrees of freedom are defined as in the previous example. Results have also been obtained in five or six

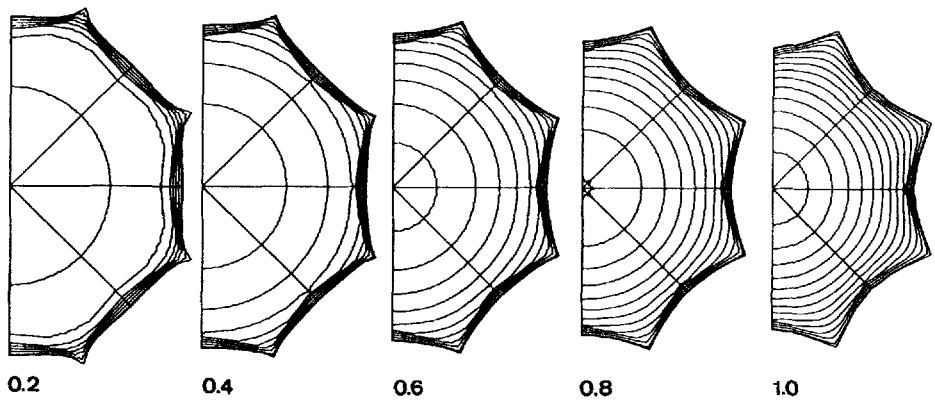

Figure 11. Die velocity profiles as a function of the power-law index for the octagonal extrudate

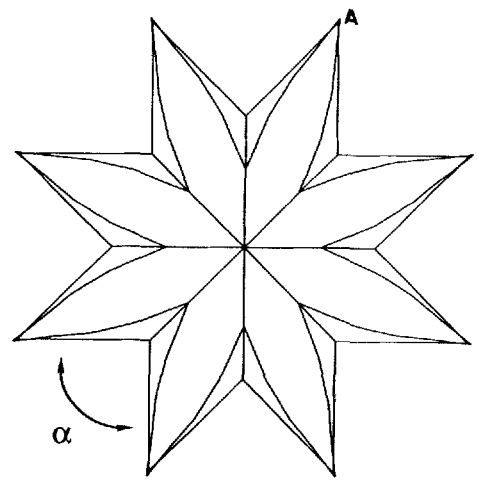

Figure 12. Die cross-section for the star-like extrudate (Newtonian fluid)

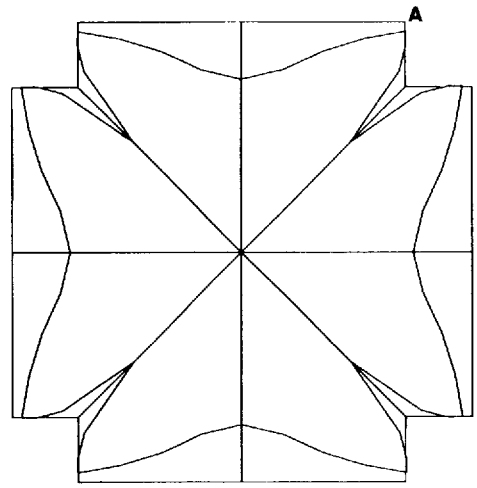

Figure 13. Die cross-section for the cross-like extrudate (Newtonian fluid)

iterations. For angles α smaller than 90° and for a Newtonian fluid we have observed difficulties in obtaining solutions to the IEP.

5.4. *Cross-like profile*

The method presented in this paper has the capability to handle profiles with multiple corners. We have therefore computed the IEP for an extrudate section which has the shape of a cross and involves 12 corners. We have also used symmetry with respect to the planes $x=0$ and $x=y$ and discontinuity of the direction **d** at the corner A. The fluid is Newtonian.

In all previous Newtonian cases we have started the Newton–Raphson scheme from a solution obtained on the fixed geometry, the normal velocity boundary condition being dropped on the free surface. In the present case divergence of the iterative scheme has been observed and we had to find an initial solution by solving three explicit iterations on the free surface position. The Newton–Raphson scheme can then be initiated and quadratic convergence is observed. The total number of iterations in order to reach a relative precision of 10^{-6} is equal to eight (three explicit iterations and five implicit iterations). A comparison between the die and extrudate shapes can be found in Figure 13. For large aspect ratios we have not been able to find a solution to the IEP with a Newtonian fluid.

6. CONCLUSIONS

We have presented a numerical scheme to solve the inverse extrusion problem by means of an implicit Newton–Raphson iterative technique. Discontinuity of the direction of displacement as well as a remeshing technique based on the Euclidean distance have been used in the extrudate section. The same remeshing technique has been used in the adaptive section of the die.

The method, which is based on an implicit formulation, avoids the 'trial-and-error' iterations classically used to solve the IEP. Therefore the cost of the IEP is (almost) identical to the cost of the DEP, the number of additional variables being only marginal.

Several profile shapes have been presented. The results show that for a Newtonian fluid with a no-slip boundary condition at the die wall the die section differs strongly from the extrudate

section. The effect of shear thinning has also been analysed for an octagonal extrudate. Although less swelling is expected for a shear-thinning fluid, results show that the die section shape still differs from the section of the extrudate, especially in the vicinity of corners.

The method can be directly extended to non-isothermal problems, while slipping at the wall can be easily introduced provided that the relationship between the shear stress and the tangential velocity is known.

ACKNOWLEDGEMENTS

V. Legat wishes to acknowledge a scholarship from the Belgian 'Fonds National de la Recherche Scientifique'. The results presented in this paper have been obtained within the framework of Interuniversity Attraction Poles initiated by the Belgian State, Prime Minister's Office, Science Policy Programming.

REFERENCES

1. T. Tran-Cong and N. Phan-Thien, 'Die design by a boundary element method', *J. Non-Newtonian Fluid Mech.*, **30,** 37–48 (1988).
2. O. Wambersie and M. J. Crochet, 'Transient finite element method for calculating steady state three-dimensional free surfaces', *Int. j. numer. methods fluids*, **14,** 343–360 (1992).
3. T. Yokoi and L. E. Scriven, 'Profile extrusion and die shape designed by Galerkin's method with streamline-adapted basis functions', *J. Non-Newtonian Fluid Mech.*, in press.
4. K. R. J. Ellwood, T. C. Papanastasiou and J. O. Wilkes, 'Three-dimensional streamlined finite elements: design of extrusion dies', *Int. j. numer. methods fluids*, **14,** 13–24 (1992).
5. B. A. Finlayson, 'Existence of variational principles of Navier–Stokes equations', *Phys. Fluids*, **15,** 963 (1982).
6. I. Babuska, 'The finite element method with Lagrangian multipliers', *Numer. Math.*, **20,** 179–192 (1973).
7. D. Berghezan and F. Dupret, 'Numerical simulation of stratified coating flow by a variational method', *J. Comput. Phys.*, in press.
8. V. Legat and J. M. Marchal, 'Prediction of three-dimensional general shape extrudates by an implicit iterative scheme', *Int. j. numer. methods fluids*, **14,** 609–625 (1992).